AIAA JOURNAL
Vol. 34, No. 9, September 1996

Spatial Evolution of Görtler Instability in a Curved Duct of High Curvature

Philippe Petitjeans* and José-Eduardo Wesfreid†
Ecole Supérieure de Physique et de Chimie Industrielles, F-75231 Paris Cedex 05, France

The Görtler instability is investigated experimentally in a water channel of high curvature. Two different kinds of experiments are presented. The first one corresponds to an experiment where the flow rate increases and where we study the instability in a given longitudinal position along the concave wall. We find a law for the full nonlinear behavior as a correlation for the velocity perturbation as a function of the Görtler number. In the second set of experiments, we follow the spatial evolution of the instability along the concave wall for a given flow rate. We observe the saturation due to the nonlinearities and to the diminution of the thickness of the boundary layer. We show the importance of the initial conditions and of the wavelength in the evolution of the instability.

I. Introduction

THE flow in curved ducts has been, and still is, investigated largely because of its fundamental interest as well as its importance in technological realizations such as heat exchangers, airfoils, turbine blades, or any part with curved surfaces. The boundary-layer flow on a concave surface can be unstable. This instability is known as the Görtler instability. It is the consequence of the imbalance between the centrifugal forces and the radial pressure gradient. It produces longitudinal rolls in counter-rotating pairs aligned in the direction of the main flow.[1-5]

On turbine blades for instance, the instability perturbs the film cooling system. This system consists of injections of colder fluid on the surface of the blade with small jets coming from the inside of the blade. On the pressure side, which corresponds to the inner portion of the blade where the surface is concave, the Görtler instability can dramatically modify the heat exchange. Also, the rotation of the blades, which adds Coriolis effects, can disturb the basic flow as well as the instability development.[6,7]

Meanwhile the Görtler vortices are the natural prototype of longitudinal organized structures arising in flows. Indeed, in the field of heat transfer, many improvements were obtained with airfoils, pins, or other vortex generators, to induce artificially longitudinal vortices in the flow. The strongly nonlinear velocity field induced with theses vortex generators produces extended regions of down wash flow towards the wall, enhancing the heat and/or mass transfer.

The Görtler instability belongs to the class of centrifugal instabilities such as the Taylor–Couette instability between two concentric cylinders in rotation or the Dean instability of a Poiseuille flow within a curved channel.[8,9] Simultaneously, it also belongs to the class of instabilities in open systems. This double character generates all of the richness (as well as the complexity) of this system.

The control parameter of this instability is the Görtler number G. Its expression is

$$G = Re(\delta/R)^{\frac{1}{2}} = (U\delta/\nu)(\delta/R)^{\frac{1}{2}}$$

where U is a characteristic velocity of the flow, δ is the thickness of the boundary layer, ν is the kinematic velocity, and R is the radius of curvature of the concave wall. This Görtler number can be interpreted as the ratio between the inertial and centrifugal effects to the viscous effects.

Received Oct. 4, 1994, revision received July 29, 1995; accepted for publication Jan. 12, 1996.

*Chargé de Recherche, Laboratoire de Physique et Mécanique des Milieux Hétérogènes, URA Centre National de la Recherche Scientifique 857, 10, rue Vauquelin.

†Directeur de Recherche, Laboratoire de Physique et Mécanique des Milieux Hétérogènes, URA Centre National de la Recherche Scientifique 857, 10, rue Vauquelin.

Aspect of Centrifugal Instability

Centrifugal instabilities appear when the curvature of the streamlines could induce longitudinal rolls. The criterion that gives a necessary condition for a centrifugal instability is the inviscid Rayleigh's criterion 8: a flow in which the Rayleigh's discriminate is negative is potentially unstable, where the Rayleigh's discriminate is written as

$$\phi(r) = \frac{1}{r^3}\frac{\mathrm{d}}{\mathrm{d}r}(rU)^2$$

In the case of a small curvature, when the characteristic length of the flow d is very small compared with the radius of curvature, the Rayleigh's discriminate can be written as

$$\phi(r) \propto U\frac{\mathrm{d}U}{\mathrm{d}r}$$

A boundary-layer flow is stable on a convex wall and potentially unstable on a concave one.

Aspect of Open Flow

The Görtler instability presents an important difference with the Taylor–Couette instability and at a lower level with the Dean instability. Indeed, in the Taylor–Couette problem the streamlines are closed on themselves and the instability appears in a confined system. Thus, a permanent feedback exists and the rolls are autoregenerated by themselves. This regeneration can explain the absolute character of the Taylor–Couette instability. In addition, the gap between the two walls remains constant. For given rotation speeds of the cylinders, the Taylor number

$$\mathrm{Ta} = (Ud/\nu)(d/R)^{\frac{1}{2}}$$

is equal to a constant value that does not change either in time or in space. When the rolls are formed, they remain at a constant amplitude in the flow, at least until a second threshold where, for example, they can oscillate. This system is spatially homogeneous. The Dean instability is not an instability in a physically closed system in the sense where the flow does not shape a loop. However, we can observe that the evolution of the thickness of the unstable region remains constant in time as well as in space (an established Poiseuille flow does not evolve along a flow). Thus, the Dean number

$$\mathrm{De} = (Ud/\nu)(d/R)^{\frac{1}{2}}$$

remains constant for a given flow in a given geometry. Nevertheless, the amplitude of the rolls that appear after the inlet of the curved section evolves along the flow in a different way to the Taylor–Couette problem, as in a typical problem of spatial instability with nonlinear saturation. The perturbations in this system are spatially inhomogeneous, even if the basic flow is spatially homogeneous.

Clearly, the Görtler instability is an open flow instability in the sense that the flow is not closed on itself as in the Taylor–Couette problem. But it is also, above all, a spatially inhomogeneous instability both in terms of perturbations and the basic flow. Indeed, the thickness of the boundary layer, corresponding to the unstable region, does not remain constant, but it evolves along the flow: $\delta = \delta(x)$. Consequently, the Görtler number, built with this characteristic length, evolves also in the streamwise direction:

$$G_\delta = \frac{U\delta(x)}{\nu}\left[\frac{\delta(x)}{R}\right]^{\frac{1}{2}} = G_\delta(x)$$

Hence, the destabilizing effects are not constant along the wall. In the spatial theory of linear stability, this particularity is manifested in an alternative way to write the Görtler number as

$$G^2 = (x/R)(Ux/\nu)^{\frac{1}{2}}$$

obtained from the explicit Blasius law on flat plate for $\delta(x)$.

Another important characteristic of an instability in an open flow is the receptivity to initial perturbations or, in other words, the absolute or convective aspect of the instability. It is generally agreed that instabilities in open flow are convective most of the time and could become absolute after a second threshold. The Görtler instability is considered as a convective instability by most of the authors who have worked on this subject.[10–18] Park and Huerre[12] deduce this from their calculations in the case of a flow with wall suction and a boundary layer of constant thickness. Chomaz[13] and Chomaz and Perrier[14] show it from preliminary experiments where they study the effects of initial perturbations. Ruban[15] has studied the case of large wavelengths with an asymptotic method in the limit of large Reynolds number and large Görtler number. He shows that the flow is absolutely unstable when it is perturbed by transversal periodic perturbations. He has also studied the case of a single point initial perturbation, and he finds that the instability is convective. Rozhko et al.[16] and Savenkov[17] have also studied this problem and have obtained the same conclusion. Choudhari et al.[18] worked on the problem of spatial evolution of the Görtler rolls in the case of large wavelengths and concluded that the instability is convective.

Recent reviews have been written on the different studies on the Görtler instability.[3–5] Most of the studies on this subject were made in the case where the curvature is small enough to use the assumption of the Blasius velocity profile as the basic profile and to neglect the effect of an eventual longitudinal pressure gradient.

We present experimental results obtained on a wall of high curvature. In this situation, it is not possible to use the same assumptions of basic Blasius profile anymore. We show the effect of the curvature on the basic velocity profile and the importance of the longitudinal pressure gradient that induces an important deviation of the evolution of the boundary layer compared with the classical Blasius profile of a flow on a flat wall. We discuss the effect of the nonparallelism of the basic flow on the spatial evolution of the rolls.

In Sec. II, we describe the experiment setup and the measurement methods we use. In Sec. III, we recall the basic velocity profile of the velocity field, in our case of a flow in a curved duct of high curvature. In Sec. IV, we present experimental results of the evolution of the instability in two important cases. In the first case, we measure the evolution of the instability at a fixed streamwise position x in the curved channel when we increase the flow rate. In the second case, we measure the spatial evolution of the rolls along the curved channel for a constant flow rate. By repetition of the same experiment, we show the effects of the uncontrolled initial perturbations on the evolution of the wavelength and the amplitude of the rolls. Then we show that both nonlinearities and decay of the thickness of the basic velocity profile produce a saturation and a diminution of the amplitude of the instability.

II. Experimental Apparatus and Procedure

We have conducted measurements in a low-velocity water channel specially built to study the Görtler instability.[19] This setup is well equipped for visualization with a system of laser-induced fluorescence using a light sheet and dye injection. Velocity measurements were made with an automatic laser Doppler anemometry (LDA) system. The setup is drawn in Fig. 1. The concave test section consists of a curved duct with a width $L_z = 10$ cm. The radius of curvature of the concave wall (outer) is $R_o = 10$ cm, and the radius of the convex wall is $R_i = 5.7$ cm. The two centers of curvature are slightly different ($d = 0.7$ cm in the horizontal direction) to

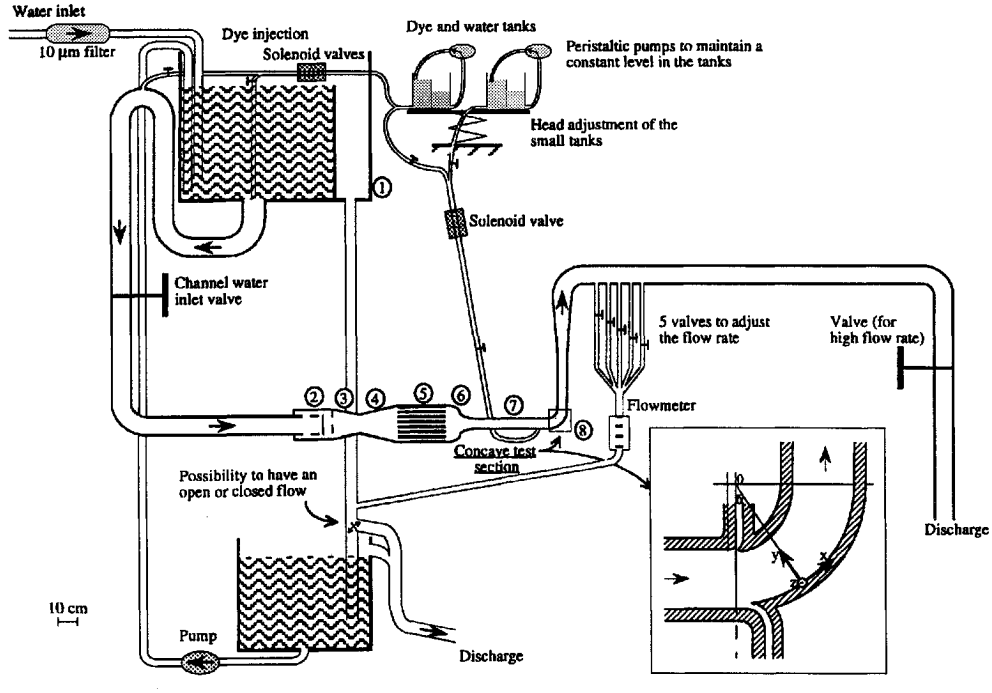

Fig. 1 Low-velocity hydrodynamic channel. The flow is generated by gravity with a constant level water tank of capacity 384 liters, located 175 cm above the channel (1). A succession of different sections makes the flow as laminar as possible: a diffuser (2), a nozzle (3), a diffuser (4), a settling chamber (5), a two-dimensional contraction chamber (6), and a relaxation section (7) where it is possible to inject dye as a sheet or several jets. The following section (8) is the curved section where we studied the Görtler instability. Then a straight section allowed us to observe the persistence of the rolls after the curved part.

compensate for the growth of the boundary layers. On each wall, there is a deviation of the flow in the inlet of the curved section to eliminate the boundary layers developing upstream.

We use the method of laser-induced fluorescence to visualize the flow and the structures generated in the curved section. We can inject dye upstream and generate a light sheet with an argon laser. The dye we use is a 0.1 g/l concentration solution of fluoresceine ($C_{20}H_{10}Na_2O_5$), so that the difference of density $\delta\rho/\rho = 10^{-4}$ is negligible. As usual, this method allows observation of structures with a vorticity orthogonal to the plan of the light sheet. Therefore, a cross section of the flow shows forms of mushrooms (Fig. 2a). We can measure the streamwise velocity field with an automatic LDA system. This system consists of a fiber-optic probe that allows for great simplicity in the placement of the point of measurement in the flow. This anemometer measures only the streamwise velocity component because it is the larger one, not only for the basic flow U, but also for the perturbation u compared with the two other components (v and w). This system is controlled by a computer that records the data. Figure 2b shows the levels of the iso-streamwise velocity field in the same cross section as the Fig. 2a. Note that the concentration field has no reason to be the same as the velocity field. Indeed, the form of the mushrooms obtained by velocimetry is different from what we observe by visualization because of the difference between the diffusion of vorticity ν and the diffusion of mass D.[20,21] The ratio is the Schmidt number $Sc = \nu/D$. This number is generally equal to 10^3 in liquids, meaning that the characteristic time of diffusion of the mass is about 1000 times larger than the characteristic time of diffusion of the vorticity. Or, in other words, the viscous boundary-layer thickness $\delta_\nu = \sqrt{(Sc)}\delta_m \approx 30\delta_m$, where δ_m is the mass boundary layer. Therefore, the visualizations in water, which show the concentration field, give forms much thinner than forms of the velocity field (in the case of gas, $Sc \approx 1$, and the profiles are closer to each other). However, visualizations give important information about the general structures of the flow, the eventual oscillations, the wavelength, etc. From these measurements, we observe the strong influence of the nonlinearities in the perturbation field. Indeed, we get a sinusoidal profile in the spanwise direction only if the nonlinearities are very weak. In that case, the inflow region and the outflow region have the same size. But it is not the case anymore in Figs. 2a and 2b. An important conclusion of this observation of the mass transfer by visualization is the consequence of the rolls on heat transfert. A passive tracer as temperature (or mass) is submitted to a higher gradient in a more extended place in the inflow region than it is in the outflow region. Hence, the heat (or mass) transfer is enhanced.

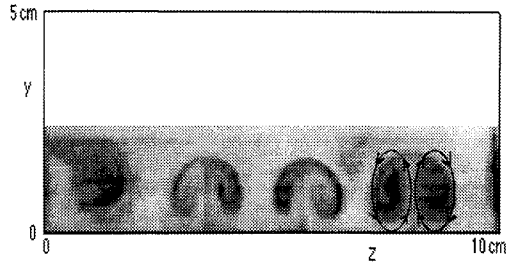

Fig. 2a Visualization of a cross section of the concave part (α = 60 deg) with a laser sheet and injection of dye upstream. The height of the picture is half of the height of the channel (2.5 cm) near the concave side, and the width is the total width (10 cm).

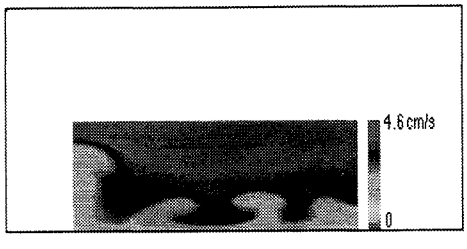

Fig. 2b Longitudinal velocity U measured by laser Doppler velocimetry in the same cross section as Fig. 3a. The light regions represent regions of high velocity, whereas the dark regions are of low velocity.

III. Basic Flow

As we explained, the concave section where we study the Görtler rolls is of high curvature (R = 10 cm). We can expect the basic flow to deviate from a Blasius profile. Indeed, we will see that both geometry and longitudinal pressure gradient produce a different evolution of the boundary layer.[22] All of the authors who have studied the Görtler instability have considered the unperturbed flow to be a Blasius profile even for small curvature,[23–25] and some of them have included the effect of a longitudinal pressure gradient. We have characterized this unperturbed flow as accurately as possible with the help of a two-dimensional numerical simulation (to avoid three-dimensional effects) to approach the two-dimensional basic flow.[22] The velocity profile is not symmetric as expected and is faster near the convex wall. This profile is the superposition of the potential profile $1/r$ (where r is the distance to the center of curvature) with the boundary layers on each wall. The boundary layer is thicker on the concave wall because the flow is slower on this side. This differs from a Blasius profile that tends to a constant value far from the wall.[22]

Now it is important to redefine some parameters such as the infinity velocity U_∞ and the displacement and momentum boundary-layer thickness. The velocity U_∞, that corresponds to the potential velocity, depends now on the distance to the center of curvature. We will use here $U_\infty = U_\infty(y)$, where y is the distance from the concave wall ($y = R - r$). We have decided to use as characteristic velocity the potential wall velocity[24] $U_{pw} = U_\infty(y = 0)$ defined as the velocity of the potential flow on the concave wall in the absence of boundary layers. We also define the thickness of the boundary layers as follows.[22]

Momentum thickness:

$$\theta = \int_0^{d/2} \frac{U(y)}{U_\infty(y)}\left[1 - \frac{U(y)}{U_\infty(y)}\right] dy$$

Displacement thickness:

$$\delta^* = \int_0^{d/2} \left[1 - \frac{U(y)}{U_\infty(y)}\right] dy$$

The upper limit of the integrals is chosen as $d/2$ (half of the channel) to avoid the influence of the convex wall. Using these definitions, we have represented in Fig. 3 an example of the spatial evolution of the thickness of the boundary layer of the basic flow on the concave wall. The evolution of the boundary-layer thickness differs from a Blasius one that evolves as $x/\sqrt{(Re)}$. We have also calculated the factor of form $H = \delta^*/\theta$. This factor is often and incorrectly used to verify if a boundary-layer profile is a Blasius profile or not. If it is, $H = \delta^*/\theta = (1.72\delta/0.664\delta) = 2.59$. Nevertheless, in our experiment, the factor of form H varies from 2.2.to 2.6 (so not very different than 2.59), but the profiles we get are not Blasius profiles.[2] Indeed, the thickness begins to increase until the boundary layer reaches a certain position along the concave wall and then

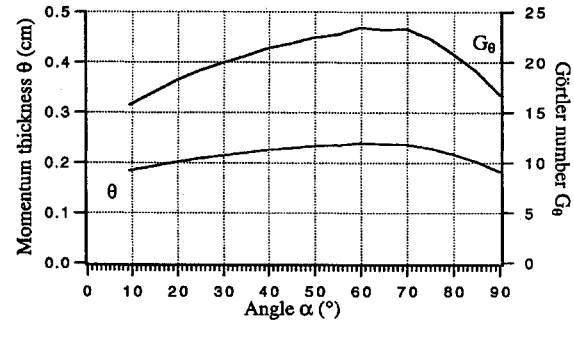

Fig. 3 Evolution of the momentum thickness θ of the boundary layer and the Görtler number G_θ along the concave wall for the profiles shown in Fig. 4.

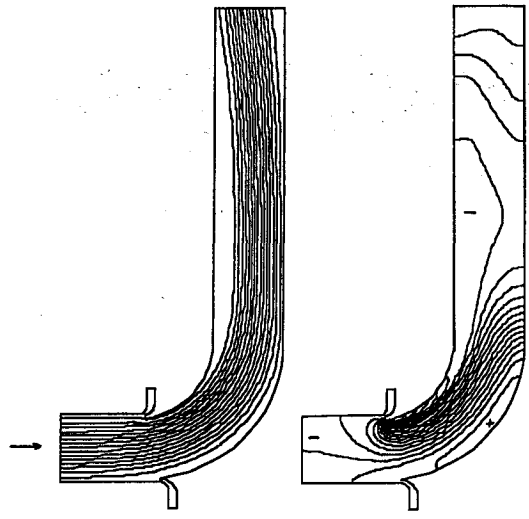

Fig. 4 Isobars and streamlines for the two-dimensional flow obtained from the numerical simulation (U_{pw} = 3.5 cm/s).

decreases. This evolution can be explained by the evolution of the pressure in the concave test section. Figure 4 represents the streamlines and the pressure obtained through the numerical simulation. There is a maximum of pressure on the concave wall near the center of the wall ($\alpha \approx 45$ deg) and lower pressure before and after. This is explained by the geometry: the tendency of a flow impinging a wall (here the region around center of the concave wall) produces a growth of the pressure on this wall. Therefore, along the concave wall, the longitudinal pressure gradient is positive until about $\alpha \approx 45$ deg and negative after this position. Consequently, in the first part of the concave section, the flow is slowed down, inducing a thickening of the boundary layer, and in the second part, the flow is accelerated, decreasing the boundary-layer thickness. This evolution of the boundary layer leads to an identical evolution of the Görtler number G_θ (Fig. 3). Hence, the decreasing of the Görtler number could be a second reason for the reduction of the amplitude of the Görtler rolls (see Sec. IV). Indeed, after about $\alpha \approx 45$ deg, the conditions are less favorable to the instability than they were in the first part of the concave section.

IV. Experimental Results

A. Experimental Procedure

Recall that we have chosen the axis as follows: x is the longitudinal axis on the concave wall ($x = R\alpha$), y is the radial one directed from the concave wall to the center of curvature, and z is the transversal one. The method we use to measure the evolution of the instability is the following. For a given longitudinal position x, we experimentally determine the streamwise velocity profile along the spanwise axis z with LDA. We observe a modulation of the streamwise velocity caused by the rolls and measure the wavelength (Fig. 5). The maximum (respective minimum) of the profile corresponds to the middle of the inflow (respective outflow) region. At these two positions, z_{inflow} and z_{outflow}, we measure the streamwise velocity profile along the radial axis y (Fig. 6). The difference between these two profiles represents the perturbations of the velocity (with a wavenumber nonzero). Indeed, the velocity is written as follows:

$$U = U_0 + u_1 \cos(2\pi z/\lambda) + \text{higher harmonic contributions}$$

where U_0 is the streamwise velocity component of the homogeneous mean flow, u_1 the perturbation at the first transversal period mode associated with the wave number $q = 2\pi/\lambda$, and λ the wavelength (Figs. 5 and 6). As soon as the velocity profile in the spanwise direction z is close to a sinusoidal profile, we can expect that the other terms $u_2, u_3, \ldots$, are not as important in comparison to u_1 as shown in the Fig. 5. In this figure, we calculate a Fourier decomposition showing that $u_2/u_1 = 0.17$ and $u_3/u_1 = 0.02$. Further work must use this kind of decomposition to quantify exactly the role of the higher nonlinear terms in the perturbation field.[26]

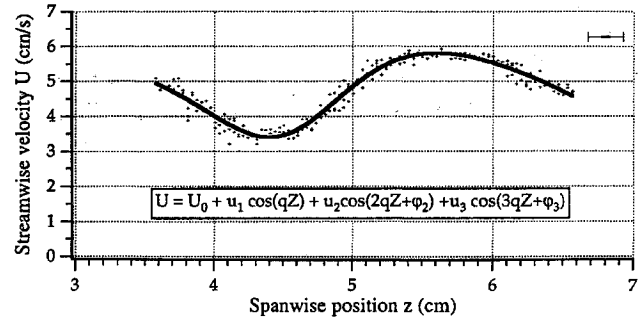

Fig. 5 Streamwise velocity U along the spanwise axis z, where α = 30 deg, y = 0.7 cm, U_{pw} = 5.6 cm/s, U_0 = 4.74 cm/s, u_1 = 1.16 cm/s, u_2 = 0.20 cm/s, u_3 = 0.03 cm/s, φ_2 = 2.37, φ_3 = 5.19, $Z = z - 2.69$, and q = 2.24.

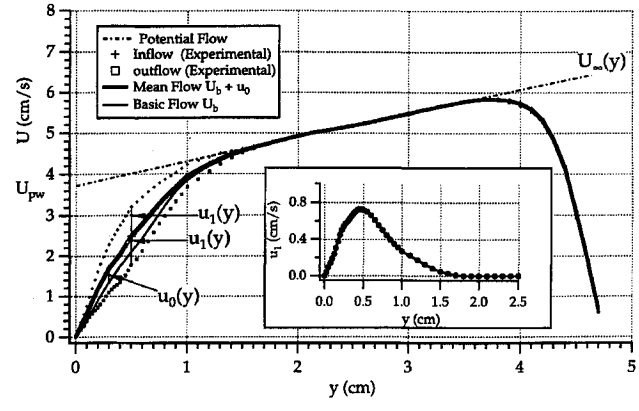

Fig. 6 Experimental streamwise velocity profile for α = 30 deg and U_{pw} = 3.72 cm/s. The streamwise perturbation u_1 is also shown.

The homogeneous mean flow is $U_0 = U_b + u_0$, where U_b is the two-dimensional basic flow and u_0 is the perturbation with a wavenumber[27] $q = 0$ usually called mean flow correction. Let us discuss briefly this unusual formulation of the homogeneous mean flow, including the zero wavenumber perturbation. In previous experimental works this possibility was not taken into account. Indeed, theoretical study on the nonlinear regime of the Görtler instability includes the existence of this mode. The mathematical origin comes from the nonlinear generation of harmonics of the spatial wavenumber. At the same level of the conditions of the existence of $2q = q + q$, the solution $0 = q - q$ is possible too.[27] This mean flow correction was detected in the Rayleigh–Benard convection[28] and theoretically analyzed by Siggia and Zippelius[29] and Hall[30] for the Taylor–Couette problem. The temporal version of this problem (the Hopf bifurcation) has been studied by Hanneman and Oertel[31] in wakes and recently in other confined flow by Pagneux and Maurel,[32] who showed the existence of a stationary perturbation of zero frequency ($\omega - \omega$) as a consequence of the instability. Recent studies of instabilities in open flows[33] show the importance of this homogeneous perturbation in the nonlinear saturation of the instabilities. Unfortunately, we cannot use the numerical simulation to calculate the basic flow for all of our experiments since it is not possible to include all of the initial perturbations (undetectable experimentally), nor the effect of Ekman cells that appear on each lateral wall, and modify the flow, especially in our relatively short cell. Therefore, we cannot detect the mean flow correction u_0 from the experimental measurements but only U_0, where $U_0 = U_b + u_0$ is the total homogeneous streamwise velocity.

To explore the evolution of the perturbations, there are two experimental possibilities. The first one is to change the flow rate, e.g., U_{pw}, staying at the same position x (cf. Sec. IV.B). The second one is to keep the same flow rate and to change the position x along the flow and thus obtain the spatial evolution of the Görtler rolls along

the flow (cf. Sec. IV.C). We characterize the perturbation u_1 by its maxima $u_{1\max}$ or by its integrated value, the rms

$$u_{1\mathrm{rms}} = \left[\frac{1}{d}\int_0^d u(y)^2\,dy\right]^{\frac{1}{2}}$$

to better take into account the entire perturbation (Fig. 6).

B. Experiment Position Fixed, Flow Rate Variable

In this experiment, we keep the position fixed along the wall $x = 5.2$ cm from the leading edge, corresponding to an angle $\alpha = 30$ deg, and to make the flow rate of the channel evolve between 780 and 1240 l/h, e.g., a potential wall velocity U_{pw} between 2.1 and 6.7 cm/s. It does not evolve and remains equal to $\lambda = 2.4$ cm (± 0.2 cm). This quasi-invariance of the wavelength with the velocity of the flow has already been observed by several authors.[1,23,34–36] In the Görtler literature, many authors use the dimensionless wavelength $\Lambda = (U\lambda/\nu)(\lambda/R)^{1/2}$. In our experiment, Λ goes from 300 to 1200. The evolution of the momentum thickness of the boundary layer and of the Görtler number are represented in the Fig. 7. The thickness of the boundary layer follows a law like $1/\sqrt{(U_{pw})}$, as in a Blasius profile, until a velocity $U_{pw} \approx 3.3$ cm/s. After that, the influence of the longitudinal pressure gradient is felt, and the thickness remains constant and then increases. Consequently, the Görtler number starts to increase with a law in $U_{pw}^{1/4}$ and then increases more rapidly. The longitudinal pressure gradient dp/dx on the wall is a linear function of the mean velocity U_{pw}, with a slope of 3.6×10^{-8} s/cm^2.

Figure 8 shows the evolution of the instability as a function of the Görtler number. We have chosen to show the rms of the perturbation $u_{1\mathrm{rms}}$. We can observe that the amplitude of the rolls increases with the velocity of the flow. The perturbation is around 8% of the potential wall velocity and is still small compared with the velocity of the flow, even so far away from the apparent critical Görtler number of this experiment (defined later). Recall that the value of the threshold, very well defined for many instabilities, has no universal signification in the case of the Görtler instability. Indeed, this instability is very sensitive to the initial perturbations (cf. Sec. IV). Consequently, it is not possible to calculate a unique critical Görtler number. There is no universal neutral curve in this problem[37] since each perturbation field in the entrance of the channel produces a different value of the critical Görtler number. The experiment presented here is for a Görtler number G_θ between 9 and 21. From

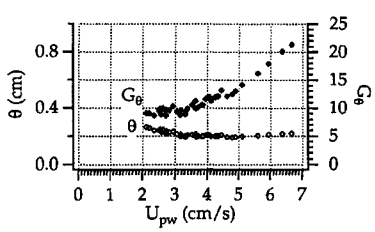

Fig. 7 Variation of the momentum thickness θ of the boundary layer and the Görtler number G_θ as function of the potential wall velocity U_{pw} for $\alpha = 30$ deg.

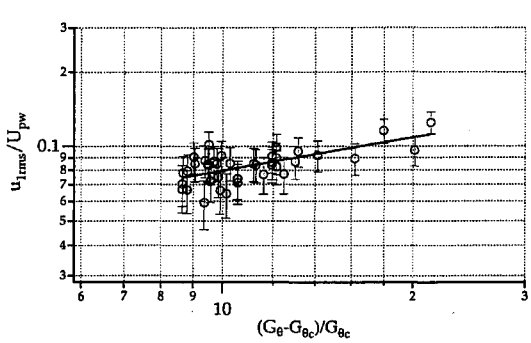

Fig. 8 Evolution of the rms of the streamwise perturbation $u_{1\mathrm{rms}}$ vs the Görtler number G_θ. The best correlation of this curve is $(u_{1\mathrm{rms}}/U_{pw}) \propto [(G_\theta - G_{\theta_c})/G_{\theta_c}]^{0.4}$ with an apparent critical Görtler number $G_{\theta c} \approx 1.6$.

this local study, we can estimate the evolution of the strength of the instability in the nonlinear range. The best fit of the data shown in Fig. 8 gives the following power law:

$$\frac{u_{1\mathrm{rms}}}{U_{pw}} \propto \left(\frac{G_\theta - G_{\theta_c}}{G_{\theta_c}}\right)^{0.4}$$

with an apparent critical Görtler number $G_{\theta c} \approx 1.6$. This is the first time that a nonlinear correlation has been observed experimentally. The Görtler number being large for this experiment, the evolution of the rolls is strongly nonlinear, and it could be the reason why the coefficient we have obtained in the correlation is different from what we would have expected from a weakly nonlinear amplitude model as the Landau–Stuart theory.[8,38] This model predicts the following values of the exponents in the law $v = (G - G_c)^\beta$: $\beta = \frac{1}{4}$ for a subcritical behavior, or $\beta = \frac{1}{2}$ for a supercritical one. A possibility to model this behavior could be to not keep the critical Görtler number constant but to consider it as a function of the velocity U_{pw}. This can be justified by considering the longitudinal pressure gradient $\partial p/\partial x = f(U_{pw})$. Under this assumption, Ragab and Nayfey[39] show that the critical Görtler number depends on the evolution of the longitudinal pressure gradient and so on the velocity of the flow, $G_{\theta c} = G_{\theta c}(U_{pw})$. Hall[37] has calculated a critical Görtler number as a function of the initial perturbations upstream that are influenced by the modification of the velocity of the flow. Nevertheless, Lee and Liu[40] and Yu and Liu[41] did not observe any significant difference in their numerical simulations when they changed the state of the initial perturbations. In our experiment, there is no way to determine the evolution of the critical Görtler number since it is very difficult to detect these initial perturbations. Future work (experimental and numerical) needs to complete and validate (or not) this correlation.

C. Experiment Position Variable, Fixed Flow Rate

The experiment described earlier is only a local study of the instability. Although it is very important to know the magnitude of the perturbation field, it is more interesting to observe the spatial evolution of the instability along the flow for a given flow rate. In particular, we want to characterize the envelope in which the Görtler rolls evolve. Indeed, other instabilities in open systems as Bénard–von-Kármán wakes or mixing layers possess analogies with our instability that we must consider.[42] One of the main characteristics of the Görtler instability is that the rolls are in the longitudinal direction where the control parameter does not remain constant. Thus, the concept of envelope of the rolls becomes important because it describes the evolution of the instability along the wall. We will try to see whether an interpretation of this instability in terms of global behavior is possible, as it seems to be in other instabilities in open flow.[43]

1. *Wavelength Variable*

The first experiment (called $\lambda_{\mathrm{variable}}$) has been obtained under the following conditions. The flow rate of the channel was $Q = 603\,1/h$ ($\pm 5\%$), corresponding to a potential wall velocity $U_{pw} \approx 3.46$ cm/s. The potential wall velocity along the concave wall starts at 3.75 cm/s, decreases to 3.25 cm/s in the middle of the wall, and then increases to 4.25 cm/s at the exit of the concave section. This evolution is a result of the effects of the longitudinal pressure gradient. The spatial evolution of the wavelength is shown in Fig. 9 with circles. We will see in this section and the following that this growth is not related to a growth in instability. Figure 10 represents the spatial evolution of the momentum thickness of the boundary layer and the Görtler number. Both increase until an angle $\alpha \approx 40$ deg and then decrease. These evolutions are a result of the behavior of the longitudinal pressure gradient that is changing sign around the middle of the (channel $\alpha \approx 40$ deg). Recall that the decay of the Görtler number means that the flow is locally less unstable, and that is another reason of the diminution of the instability that we will observe in the next figure. Indeed, Fig. 11 shows the evolution of the rms of the longitudinal perturbation u_1. First, we observe an exponential growth of the perturbation along the wall until an angle $\alpha \approx 40$ deg. This growth can be written $u_{1\mathrm{rms}} \sim e^{\beta x}$ where β is the spatial linear growth rate. For this experiment, we find $\beta \cdot \theta_m \approx 1$, where θ_m is the mean value of the boundary-layer thickness ($\theta_m \approx 0.22$). In addition, we observe

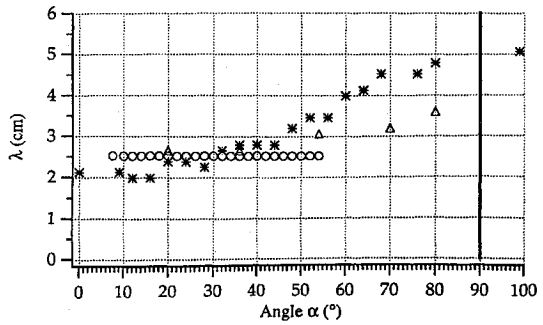

Fig. 9 Evolution of the wavelength λ along the concave wall for the three experiments: *, for the experiment called $\lambda_{variable}$; Δ, for the experiment $\lambda_{quasiconstant}$; and o, for the experiment λ_{forced}.

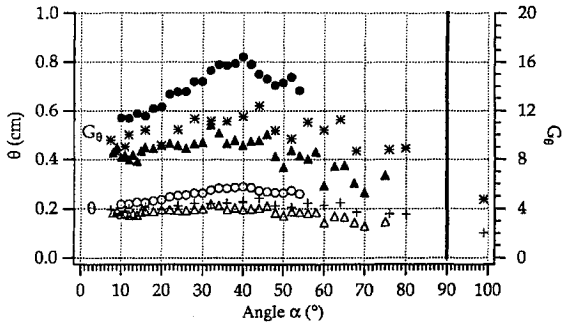

Fig. 10 Evolution of the momentum thickness θ of the boundary layer and the Görtler number G_θ along the concave wall for the three different experiments: *, for the experiment called $\lambda_{variable}$; Δ, for the experiment $\lambda_{quasiconstant}$; and o, for the experiment λ_{forced}.

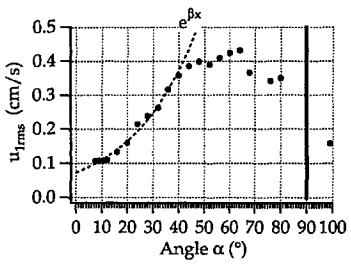

Fig. 11 Evolution of the rms of the streamwise perturbation u_{1rms} along the concave wall for the experiment $\lambda_{variable}$. Until $\alpha \approx 40$ deg, u_{1rms} grows exponentially with a law $u_{1rms} \approx 7.25\,10^{-2} e^{\beta x}$ with $\beta \approx 0.23$ and then saturates.

that the perturbation does not start at zero at the inlet of the concave section ($\alpha = 0$ deg). This can be explained by the nonzero perturbation rate in our channel. Then, after $\alpha \approx 40$ deg, the perturbation slows down its growth until an angle $\alpha \approx 64$ deg, and after this position, it decreases. This saturation of the instability is, for one part, a result of the nonlinear effects and, for another part, the local decay of the Görtler number, and hence the decay of the motor for the instability. This form of envelope of the instability is very similar to that obtained by Saric[5] and Benmaleck[43] in the nonlinear calculations of the Görtler instability. First, they calculate an exponential evolution of the energy of the rolls and then a saturation caused by the nonlinearities. In our case, the decay of the thickness of the boundary layer, and hence the decay of the Görtler number, enhances the saturation.

2. Wavelength Constant or Quasiconstant

We have run two other experiments under the same external flow conditions to study the repeatability of the evolution of the Görtler instability with different perturbations and wavelengths. Indeed, this instability, as well as almost all convective instabilities in open flow, is very sensitive to the initial perturbations. The first one is under the same conditions, as best as it is possible to get identical conditions in an experiment. This means that we can control only the flow rate with reasonable accuracy, but we do not have any control on the initial perturbations that always exist in an experiment. The second one is under the same external conditions of flow, but with injections of two small jets 5 cm before the inlet of the channel. The aim of these two jets is to impose a constant wavelength $\lambda = 2.5$ cm corresponding to the mean wavelength we have measured in the experiment described in Sec. IV.C.1. Jets present the double interest of forcing the instability and forcing the wavelength. Indeed, a jet induces two counter-rotating rolls aligned in the streamwise direction[44] and two other smaller rolls as a result of the stretching of the vorticity of the boundary layer created by the presence of the obstacle formed by the jet (Fig. 12). Therefore, it is one of the best initial perturbation to force Görtler rolls. The potential wall velocity is the same for all three experiments, confirming that, at least for the mean flow, the experiments are run under the same conditions. Figure 9 shows the evolution of the wavelengths along the concave wall. We observe three different situations. The experiment with the injection of two jets has a wavelength equal to the distance between the jets. The other experiment without jets, which was as close as possible to the experiment described in Sec. IV.C.1, had a wavelength that increases from 2.6 to 3.5 cm. In what follows, we will call the experiment described in Sec. IV.C.1 experiment $\lambda_{variable}$, the experiment where the wavelength does not evolve a lot experiment $\lambda_{quasiconstant}$, and the experiment with the two jets experiment λ_{forced}. The differences between the experiment $\lambda_{variable}$ and the experiment $\lambda_{quasiconstant}$ are the spatial distribution of the initial pertubations with approximately the same amplitude. Here, we observe how important these initial perturbations, which we cannot control in an experiment or in a real application, can be. Figure 10 shows the spatial evolution of the momentum thickness of the boundary layer and the Görtler number. The evolutions are qualitatively the same for the three experiments. The quantitative difference for the experiment λ_{forced} is a result of the jets and the rolls they induce. The evolution of the amplitude of the rolls is represented in Fig. 13. In the three cases, the amplitude of the rolls increases and decreases downstream. But the position of the maximum is not the same for all of the experiments. The maximum of the longitudinal perturbation corresponds to an angle $\alpha = 64$ deg (±2 deg) for the experiment $\lambda_{variable}$, $\alpha = 46$ deg (±2 deg) for the experiment $\lambda_{quasiconstant}$, and $\alpha = 38$ deg (±2 deg) for the experiment λ_{forced}. Hence, the saturations are very different, depending on the

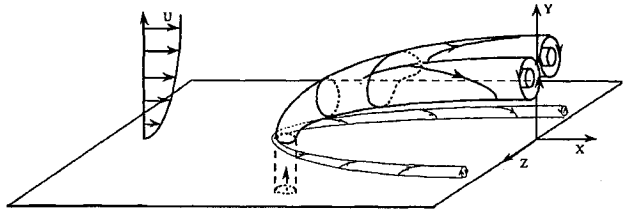

Fig. 12 Schema of a jet in a flow that produces two longitudinal counter-rotating rolls and two small rolls on the wall that disappear slowly.

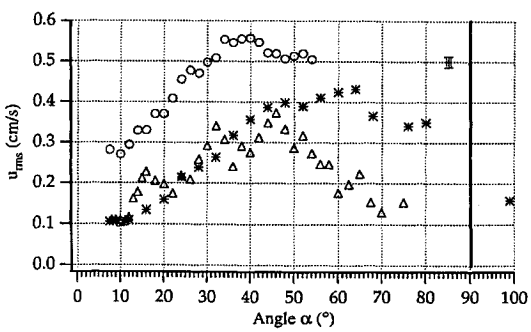

Fig. 13 Evolution of the rms of the streamwise perturbation u_{1rms} along the concave wall for the three different experiments: *, for the experiment called $\lambda_{variable}$; Δ, for the experiment $\lambda_{quasiconstant}$; and o, for the experiment λ_{forced}.

experiments. This behavior of the saturation changing with the wavelength has been observed by Day et al.[45] in their calculations of the spatial linear stability. They also observe that the higher the wavelength, the farther downstream the position of the saturation occurs. In other respects, the rms of the initial perturbation that enters in the concave section is about the same for the experiment $\lambda_{\text{quasiconstant}}$ and the experiment $\lambda_{\text{variable}}$. On the other hand, it is very different for the experiment λ_{forced}, which is about 3.5 times bigger. This is obviously a result of the jets that inject energy in the rolls. Hence, it seems that the nonlinear saturations appear later when the wavelength is free to growth to a big value. In other words, the nonlinearities are very dependent on the wavelength of the Görtler rolls and their evolution, as well as on the initial conditions that play a big part in their evolution.

Another point to observe is the serrated evolution of the experiment $\lambda_{\text{quasiconstant}}$. This can be the signature of a stationary secondary instability. This seems to be a symmetric or varicose instability, with a wavelength $p_x \approx 2.8$ cm.

V. Conclusion

This work is the first quantitative experimental study of the full nonlinear behavior of the Görtler instability. The modern experimental methods used have allowed us to get a very important quantity of data to scan the velocity field in all of the curved section. These data could be compared with results obtained with new powerful codes of direct simulation of the Navier–Stokes equations. On account of the curvature, which is much higher than almost all of the other work, and of the longitudinal pressure gradient, the basic profile is not a Blasius boundary-layer profile any more: the thickness of the boundary layer starts to increase in the first halfway of the concave section and then decreases. Consequently, we have shown that this evolution has to be taken into account in the evolution of the rolls, in particular, in the saturation of the instability. From the experiment in a fixed position with a variable flow rate, we have gotten a correlation of the strength of the instability. From the other experiments where we have measured the spatial evolution of the Görtler rolls, we have shown the importance of the initial perturbation and the behavior of the wavelength in all of the development of the instability. Our experiments show the limits of validity of the linear description of the instability about the importance of the nonlinear description of the Görtler vortices.[46] In that sense, the Görtler instability becomes a good subject of study, not only as a centrifugal instability, but also as a model of open and convective flow, where the nonparallel effects are important. In this paper, we have shown the importance of the mean flow correction even if we were not able to extract this component. We know that this component plus the other nonlinear components are responsible for the enhancement of heat transfer. An important research direction in the future will be the study of these nonlinear corrections in experiments and direct numerical simulations.[47]

Acknowledgments

The first author has been supported by the Société Nationale d'Etude et de Construction de Moteurs d'Avions (SNECMA) and the Association Nationale de la Recherche Technique (Convention Industrielle de Formation par la Recherche 481-89), and the work has been supported by the SNECMA and the Centre National de la Recherche Scientifique. We acknowledge H. Peerhossaini for helpful discussion.

References

[1]Swearingen, J. D., and Blackwelder, R. F., "The Growth and Breakdown of Streamwise Vortices in the Presence of a Wall," *Journal of Fluid Mechanics*, Vol. 182, Sept. 1987, pp. 255–290.

[2]Petitjeans, P., "Etude expérimentale des instabilités de couches limies sur des parois concaves: Instabilité de Görtler," Thése, Dept. de Mécanique, l'Université Paris VI, Paris, 1992.

[3]Peerhossaini, H., and Wesfreid, J. E., "On the Inner Structure of Streamwise Görtler Rolls," *International Journal of Heat and Fluid Flow*, Vol. 9, No. 1, 1988, pp. 12–18.

[4]Floryan, J. M., "On the Görtler Instability of Boundary Layers," *Progress in Aerospace Sciences*, Vol. 28, 1991, pp. 235–271.

[5]Saric, W. S., "Görtler Vortices," *Annual Review of Fluid Mechanics*, Vol. 26, 1994, pp. 379–409.

[6]Aouidef, A., Wesfreid, J. E., and Mutabazi, I., "Coriolis Effects on the Görtler Vortices in the Boundary Layer Flow on Concave Wall," *AIAA Journal*, Vol. 30, No. 11, 1992, pp. 2779–2782.

[7]Pexieder, A., Truong, T. V., and Maxworthy, T., "Velocity Measurements, Using DPIV, of Görtler Flows with System Rotation," *Proceedings of the Euromech No. 327 Colloquium on Effects of Organized Vortex Motion on Heat and Mass Transfer* (Kiev), edited by H. Peerhossaini and N. Yurchenko, 1994, p. 14.

[8]Drazin, P. W., and Reid, W. H., *Hydrodynamic Stability*, Cambridge Univ. Press, New York, 1981, Chap. 3.

[9]Chandrasekhar, S., *Hydrodynamic and Hydromagnetic Stability*, Dover, New York, 1981.

[10]Huerre, P., "Spatio-Temporal Instabilities in Closed and Open Flows," *Instabilities and Nonequilibrium Structures II*, edited by E. Tirapegui and D. Villarroel, Kluwer, Dordrecht, The Netherlands, 1986, pp. 141–177.

[11]Bottaro, A., "Spatially Developing Flow in Curved Duct," *Proceedings of the Seventh International Conference on Numerical Methods in Laminar and Turbulent Flow*, Vol. 8, Pt. 1, edited by C. Taylor, J. H. Chin, and G. M. Homsy, Pineridge, Swansea, England, UK, 1991, pp. 696–706.

[12]Park, D., and Huerre, P., "Primary and Secondary Instabilities of the Asymptotic Suction Boundary Layer on a Curved Plate," *Journal of Fluid Mechanics*, Vol. 283, Jan. 1995, pp. 249–272.

[13]Chomaz, J. M., "Absolute and Convective Instabilities in Nonlinear Systems," *Physical Review Letters*, Vol. 69, Sept. 1992, pp. 1931–1934.

[14]Chomaz, J. M., and Perrier, M., "Nature of the Görtler Instability: A Forced Experiment," *The Geometry of Turbulence*, edited by E. J. Jimenez, Plenum, New York, 1991, pp. 23–32.

[15]Ruban, A. I., "Propagation of Wave Packets in the Boundary Layer on a Curved Surface," *Izvestiya Akademii Nauk SSSR, Mekhanika Zhidkosti i Gaza*, Vol. 2, March–April 1990, pp. 59–68.

[16]Rozhko, S. B., Ruban, A. I., and Timoshin, S. N., "Interaction of a Three-Dimensional Boundary Layer with an Extensive Obstacle," *Mekhanika Zhidkosti i Gaza*, Vol. 1, Jan.–Feb. 1988, pp. 39–48.

[17]Savenkov, I. V., "Instability of the Boundary Layer on a Curved Surface," *Mekhanika Zhidkosti i Gaza*, Vol. 1, Jan.–Feb. 1990, pp. 176–179.

[18]Choudhari, M., Hall, P., and Streett, C., "On the Spatial Evolution of Long-Wavelength Görtler Vortices Governed by a Viscous-Invicid Interaction," NASA CR 189681, Inst. for Computer Applications in Science and Engineering, ICASE Rept. 92-31, July 1992.

[19]Peerhossaini, H., "L'instabilite d'uné couche limite sur une paroi concave," Thèse d'Etat, Dept. de Mécanique, Université Pierre et Marie Curie, Paris, 1987.

[20]Petitjeans, P., and Wesfreid, J. E., "Structure and Perturbation in Görtler Vortex Flow," *Ordered and Turbulent Patterns in Taylor-Couette Flow*, edited by D. Andereck and F. Hayot, Plenum, New York, 1992, pp. 245–251.

[21]Liu, J. T. C., and Sabry, A. S., "Concentration and Heat Transfer in Nonlinear Görtler Vortex Flow and the Analogy with Longitudinal Momentum Transfer," *Proceedings of the Royal Society of London, Series A: Mathematics and Physical Science*, Vol. 432, Jan. 1990, pp. 1–12.

[22]Petitjeans, P., Wesfreid, J. E., Deplano, V., and Vlad, G., "Effect of Curvature on the Velocity Profile and Boundary Layer in Flow Through a Curved Channel," *La Recherche Aérospatiale*, Vol. 2, March 1995, pp. 125–138.

[23]Bippes, H., "Experimentelle untersuchung des laminar-turbulenten umschlgs an einer parallel angeströmten konkaven wand," Sitzungsberichte der Heidelberger Akademie der Wissenschaften Mathematisch-naturwissenschaftliche Klasse, Jahragang, 3 Abhandlung, 1972, pp. 103–180; see also NASA TM-75243, March 1978.

[24]Winoto, S. H., and Crane, R. I., "Vortex Structure in Laminar Boundary Layers on Concave Wall," *International Journal of Heat and Fluid Flow*, Vol. 2, No. 4, 1980, pp. 221–231.

[25]Crane, R. I., and Sabzvari, J., "Laser-Doppler Measurements of Görtler Vortices in Laminar and Low Reynolds Number Turbulent Boundary Layer," *Laser-Doppler Anemometry in Fluid Mechanics*, edited by R. J. Adrian, Ladaon, Instituto Superior Técnico, Lisbon, Portugal, 1984, pp. 19–35.

[26]Peerhossaini, H., and Bahri, F., "Experiments on Fourier Expansion Description of Velocity in Görtler Vortex Flow," *Bulletin of the American Physical Society*, Vol. 40, Nov. 1995, p. 1957.

[27]Smith, S. T., and Haj-Hariri, H., "Görtler Vortices and Heat Transfer: A Weakly Nonlinear Analysis," *Physics of Fluids A*, Vol. 5, Nov. 1993, pp. 2815–2528.

[28]Newell, A., Passot, T., and Lega, J., "Order Parameter Equation for Patterns," *Annual Review of Fluid Mechanics*, Vol. 25, 1993, pp. 399–453.

[29]Siggia, E. D., and Zippelius, A., "Pattern Selection in Rayleigh-Bénard Convection Near Threshold," *Physical Review Letters*, Vol. 47, No. 12, 1981, pp. 835–841.

[30]Hall, P., "Evolution Equations for Taylor Vortices in the Small-Gap Limit," *Physical Review A: General Physics*, Vol. 29, May 1984, pp. 2921–2923.

[31]Hanneman, K., and Oertel, H., "Numerical Simulation of the Absolute and Convectively Unstable Wake," *Journal of Fluid Mechanics*, Vol. 199, Feb. 1989, pp. 55–58.

[32]Maurel, A., Pagneux, V., and Wesfreid, J. E., "Mean-Flow Correction as Non-Linear Saturation Mechanism," *Europhysics Letters*, Vol. 32, No. 3, 1995, pp. 217–222.

[33]Dusek, J., Legal, P., and Fraunié, P., "A Numerical and Theoretical Study of the First Hopf Bifurcation in a Cylinder Wake," *Journal of Fluid Mechanics*, Vol. 264, April 1994, pp. 59–80.

[34]Tani, I., and Sakagami, J., "Boundary Layer Instability at Subsonic Speeds," *Proceedings of the International Council of Aerospace Sciences*, Third Congress, Stockholm, Sweden, 1962, pp. 391–403.

[35]Ito, A., "Visualization of Boundary Layer Transition Along a Concave Wall," *Flow Visualization IV (Proceedings of the 4th International Symposium on Flow Visualization)*, edited by C. Véret, Hemisphere, Washington, DC, 1987, pp. 339–344.

[36]Kottke, V., "On the Instability of Laminar Boundary Layer Along Concave Wall Towards Görtler Vortices," *Propagation and Nonequilibrium Systems*, edited by J. E. Wesfreid, H. R. Brand, P. Manneville, G. Albinet, and N. Bocvara, Springer–Verlag, Berlin, 1988.

[37]Hall, P., "The Linear Development of Görtler Vortices in Growing Boundary Layers," *Journal of Fluid Mechanics*, Vol. 130, May 1983, pp. 41–58.

[38]Manneville, P., *Dissipative Structures and Weak Turbulence*, Academic, New York, 1990.

[39]Ragab, S. A., and Nayfeh, A. H., "Effect of Pressure Gradients on Görtler Instability," AIAA Paper 80-1377, July 1980, pp. 4–15.

[40]Lee, K., and Liu, J. T. C., "On the Growth of Mushroomlike Structures in Nonlinear Spatially Developing Görtler Vortex Flow," *Physics of Fluids A*, Vol. 4, April 1991, pp. 95–103.

[41]Yu, X., and Liu, J. T. C., "On the Mechanism of Sinuous and Varicose Mode in Three-Dimensional Viscous Secondary Instability of Nonlinear Görtler Rolls," *Physics of Fluids A*, Vol. 6, No. 2, 1994, pp. 736–750.

[42]Goujon-Durand, S., Jenffer, P., and Wesfreid, J. E., "Downstream Evolution of the Bénard-von-Karman Instability," *Physical Review E*, Vol. 50, 1994, pp. 308–313.

[43]Benmaleck, A., "Nonlinear Development of Görtler Vortices over Variable Curvature Walls," Ph.D. Thesis, Dept. of Mechanical and Aerospace Engineering, Arizona State Univ., Tempe, AZ, 1993.

[44]Andreopolous, J., and Rodi, W., "Experimental Investigation of Jets in a Crossflow," *Journal of Fluid Mechanics*, Vol. 168, July 1986, pp. 393–413.

[45]Day, H. P., Herbert, T., and Saric, W. S., "Comparing Local and Marching Analyses of Görtler Instability," *AIAA Journal*, Vol. 28, No. 6, 1990, pp. 1010–1015.

[46]Bottaro, A., and Klingmann, G. B. G., "On the Linear Breakdown of Gortler Vortices," *European Journal of Mechanics B/Fluids* (to be published).

[47]Aider, J. L., and Wesfreid, J. E., "Characterization of Longitudinal Görtler Vortices in a Curved Channel Using Ultrasonic Doppler Velocimetry and Visualization," *Journal de Physique* (Paris) (to be published).